ELSEVIER

Advances in Engineering Software 31 (2000) 347–353

ADVANCES IN ENGINEERING SOFTWARE

www.elsevier.com/locate/advengsoft

A closed form for low-order panel methods

J. D'Elía[a,b,*], M. Storti[b], S. Idelsohn[b]

[a]Centro Internacional de Métodos Numéricos en Ingeniería (CIMNE), Módulo C1, Campus Norte UPC, Gran Capitán s/n, 08034 Barcelona, Spain
[b]Centro Internacional de Métodos Computacionales en Ingeniería (CIMEC), INTEC (UNL-CONICET). Güemes 3450 (3000), Santa Fe, Argentina

Accepted 18 November 1999

Abstract

A closed form for the computation of the dipolar and monopolar influence coefficients related to a low-order panel method is shown. The flow problem is formulated by means of a three-dimensional potential model; the method of discretization is based on the Morino formulation for the perturbation velocity potential. On the body surface this representation reduces to an integral equation with the source (or monopolar) and the doublet (or dipolar) densities. The former is found by application of the boundary condition, and the latter is the unknown over the surface of the body. The lower panel method is used for the analytical integrations of the monopolar and dipolar influence coefficients, with special attention to avoid a logarithmic singularity in the monopolar matrix when flat fairly structured meshes that are common in ship-wave calculations are used. © 2000 Elsevier Science Ltd. All rights reserved.

Keywords: Potential flows; Closed forms; Low-order panel methods; Singularity subtraction

1. Introduction

Panel methods are well known and widely accepted in aerospace [1,2] and in naval industry [3,4] for calculating potential flows. In some problems a two-dimensional approach is sufficient, for instance, flows past multicomponent airfoils, infinite cascade, ground effects and wind tunnels [5,6] whereas in other cases a three-dimensional approach is necessary. There exist many types of panel methods for the last case. For exterior potential flows without a free surface, three types of singularity, or surface density, can be used in the numerical solution: only-sources (monopoles), only-dipoles (dipoles) or mixed distributions. For non-lifting flows only-sources may be used, while a lift requires the third type. All these take about the same computational effort. However, as Hunt [2] states, the choice of mixed distributions leads to better results than only-source or only-dipole distributions, as it reduces leakage considerably. Most panel codes originate from the very well known Hess and Smith [7] method, see Refs. [1,2,8]. In practice, the body surface is approximated by quadrilateral or triangular panels. The zero-order methods use plane panels with a constant surface density, while in higher order methods the panels may be curved and the surface density varied in some prescribed manner [9]. The most widely used technique for ship-like problems, is the so-called Rankine source method, which is extensively reviewed in Refs. [3,10,11]. Most Rankine source methods originate from the Hess and Smith method where both the body surface and the free surface are discretized. A successful way of incorporating the free surface boundary condition, which was obtained from a so-called double model solution, was proposed by Dawson [12]. The kinematic boundary condition on the body surface specifies zero normal velocity, which is equivalent to setting the normal derivative of the velocity potential to zero, i.e. a Neumann boundary condition. An alternative formulation for a closed body is to set the potential equal to a constant inside the body surface, i.e. a Dirichlet boundary condition. An overview of the latter approach is shown in Ref. [1]. For the linear, three-dimensional, zero-speed problem of a vessel in sinusoidal waves using panel methods see Refs. [13–17]. For the solution in the time domain and the propeller problem in unsteady flow see Refs. [18–23]. The Morino [24,25] approach is a mixed formulation that involves the computation of surface integrals with both monopolar and dipolar kernels. These surface integrals can be obtained with the aim of closed or numerical integration formulas. Closed formulas are only available for low-order panel formulations and can be obtained with several approaches [7,26,27]. In the Medina and Ligget [27] approach, the surface integral over each flat panel is replaced by its closed contour integration, and a local side tern is used for each side contribution, so it can be seen as a rotational tern strategy. When this strategy is

* Corresponding author. CIMEC, INTEC (UNL-CONICET) 3450 3000 Güemes, Santa Fe, Argentina.
E-mail address: jdelia@venus.arcride.edu.ar (J. D'Elía).

0965-9978/00/$ - see front matter
PII: S0965-9978(99)00060-5

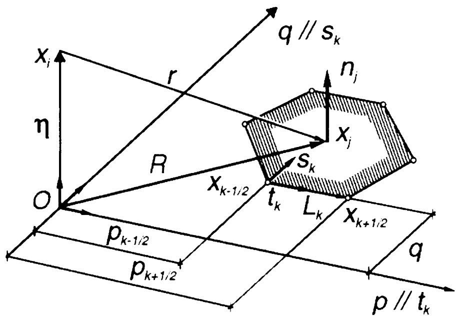

Fig. 1. Local side tern $pq\eta$ on the L^k side.

employed for panels with constant dipolar and monopolar surface layers, or panels of zero order, a singularity appears in rather special situations, for instance, in flat structured meshes that often appear in ship-wave calculations. In previous works we have considered alternative methods for potential flows with a free surface, as the ship-wave resistance problem [27–31]. In this case, we need to compute the basic flow over a reference plane, such as the hydrostatic equilibrium plane, with a fairly structured panel mesh due to some properties of the Dawson approach, but in such cases the monopolar integral can be ill-conditioned or undefined since a logarithmic singularity occurs. In this work we show in detail the rotational methodology for zero-order panels, where the logarithmic singularity is eliminated by means of a singularity subtraction.

2. Potential formulation review

Consider the flow around a body in an unbounded flow at constant speed. The fluid occupies the unbounded region Ω exterior to the wetted surface of the body Γ_S. The x-axis is parallel to the upstream non-perturbed velocity $\mathbf{u}_\infty$, the z-axis positive upwards. The potential velocity field $\mathbf{u}$ is given by $\mathbf{u} = \nabla\boldsymbol{\Phi}$, where $\boldsymbol{\Phi}$ is the total potential, which satisfies the Laplace equation in the flow region Ω and can be split as $\boldsymbol{\Phi} = \mathbf{u}_\infty^T\mathbf{x} + \phi$ where $\mathbf{x} = (x, y, z)$ is the position vector and ϕ is the perturbation potential. The kinematic boundary condition is the slip condition $\partial_n\boldsymbol{\Phi} = 0$ at the wetted body surface whereas at infinity the perturbation velocity potential tends to zero for external flows, i.e. $\phi(\mathbf{x}) \to 0$ for $|\mathbf{x}| \to \infty$. Then, the governing equations for the solution $\boldsymbol{\Phi}$ of the potential flow model are:

$$\begin{aligned} &\Delta\boldsymbol{\Phi} = 0 \ \text{ in } \Omega; \qquad \partial_n\boldsymbol{\Phi} = 0 \ \text{ at } \Gamma_S; \\ &\boldsymbol{\Phi} \to \mathbf{u}_\infty^T\mathbf{x} \ \text{ for } |\mathbf{x}| \to \infty. \end{aligned} \tag{1}$$

3. Panel formulation

The panel mesh considered here employs a low-order representation of the body surface by means of a polyhedral with n flat surfaces over the wetted body surface. We employ a low-order panel formulation, with collocation at the centroids of the panels, to set up a discrete linearized system of algebraic equations, where the system matrix is square of dimension $N = n$. The equation system of the panel method for the flow problem can be written as, $\mathbf{H}\boldsymbol{\mu} = \mathbf{b}$, where $\mathbf{H}$ is the matrix system, $\boldsymbol{\mu} = -\boldsymbol{\phi}$ is the basic bipolar vector evaluated at the centroids of the N-panels, equal to minus the basic potential vector $\boldsymbol{\phi} = [\ldots\phi(\mathbf{x}_i)\ldots]^T$ and $\mathbf{b}$ the source vector. The matrix system is the sum $\mathbf{H} = 1/2\mathbf{I} + \mathbf{A}$, of the scaled identity matrix $\mathbf{I}$ and the bipolar influence matrix $\mathbf{A}$. The source vector $\mathbf{b} = \mathbf{C}\boldsymbol{\sigma}$, is the product of the monopolar influence matrix $\mathbf{C}$ and the flow vector $\boldsymbol{\sigma} = [\ldots\sigma(\mathbf{x}_i)\ldots]^T$, obtained by means of the slip condition on the solid walls where the normal velocity component is null $\sigma(\mathbf{x}_j) = -\mathbf{u}_0^T(\mathbf{x}_j)\mathbf{n}(\mathbf{x}_j)$ for $j = 1, 2, \ldots, N$, where $\mathbf{n}(\mathbf{x}_j)$ is the j-unit panel oriented normal to the wetted side, so it can be seen as a *kinematic* source vector. The bipolar and monopolar influence coefficients A_{ij}, C_{ij} are given by the surface integrals

$$A_{ij} = \frac{1}{4\pi}\int_\Gamma \mathrm{d}\Gamma_j \frac{\mathbf{r}_{ij}^T\mathbf{n}_j}{r_{ij}^3} \qquad \text{and} \qquad C_{ij} = \frac{1}{4\pi}\int_\Gamma \mathrm{d}\Gamma_j \frac{1}{|\mathbf{r}_{ij}|}$$

$$\text{for} \qquad i, j = 1, 2, \ldots, n; \tag{2}$$

where $\mathbf{n}_j$ is the panel unit normal oriented to the wetted side, $\mathbf{r}_{ij} = |\mathbf{x}_i - \mathbf{x}_j|$ is the distance between the centroid $\mathbf{x}_i$ and the integration point $\mathbf{x}_j$ over the j-panel surface with $\mathbf{x} = (x, y, z)$, where both influence matrices $\mathbf{A}$ and $\mathbf{C}$ are dense and non-symmetric in general.

4. Monopolar matrix

For the monopolar matrix $\tilde{C}_{ij}$, we suppose a flat panel of M sides and we consider the integral

$$\tilde{C}_{ij} = \int_{S_j} \mathrm{d}S \frac{1}{r} \tag{3}$$

where $\tilde{C}_{ij} = C_{ij}/4\pi$, S_j is the j-panel surface and r the length between the collocation point $\mathbf{x}_i$ and the integration point y over the panel surface, see Fig. 1. We employ the Medina and Ligget strategy [27], where we find an auxiliary function $V(R, \eta)$ such that its bidimensional Laplacian $\Delta_{pq}V$ over the panel surface is equal to the monopolar kernel $1/r$, i.e.

$$\Delta_{pq}V = \frac{1}{r}; \tag{4}$$

with $r = \sqrt{R^2 + \eta^2}$, where $R = \sqrt{p^2 + q^2}$ is the projection of the position vector $\mathbf{r}$ over the panel plane and η the length between the collocation point $\mathbf{x}_i$ and the plane (constant). Then, we convert the surface integral into a line integral by means of the 2D-divergence theorem

$$\tilde{C}_{ij} = \int_{S_j} \Delta_{pq}V \, \mathrm{d}S_{pq} = \int_{L_j} (\nabla_{pq}V, \mathbf{s}) \, \mathrm{d}L; \tag{5}$$

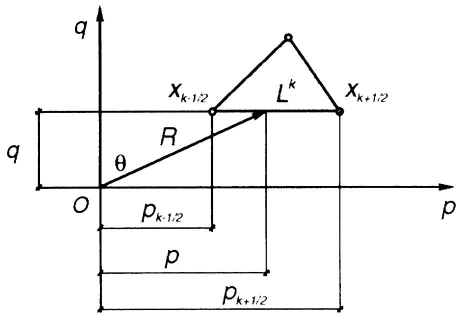

Fig. 2. The pq-plane on the L^k local side.

where $\mathbf{s}$ is the planar normal unit to the sides L_j, Δ_{pq} is the planar Laplacian operator in the p, q-coordinates and $V(R,\eta)$ a regular function, The auxiliary monopolar function $V(R,\eta)$ is found solving the differential equation

$$\frac{1}{R}\frac{\partial}{\partial R}\left(R\frac{\partial V}{\partial R}\right) = \frac{1}{\sqrt{R^2+\eta^2}}; \tag{6}$$

where $\Delta_{pq}V$ is the bidimensional Laplacian in the R,θ polar coordinates, with $\partial_\theta V = 0$. The integration process gives

$$V = \int \frac{\sqrt{R^2+\eta^2}}{R}\,\mathrm{d}R; \tag{7}$$

which admits the solution [32]:

$$V(R,\eta) = \sqrt{R^2+\eta^2} + |\eta|\ln\left[\frac{\sqrt{R^2+\eta^2}-|\eta|}{R}\right] \tag{8}$$

for $R > 0$;

where the logarithm argument is positive for R, η positives. Then, the line integral for the monopolar coefficient $\tilde{C}_{ij}$, can be written as the sum of the $\tilde{C}^k$ contributions of the surface gradient of the auxiliary monopolar function V:

$$\tilde{C}_{ij} = \sum_{k=1}^{M}\tilde{C}_k \qquad \text{where} \qquad \tilde{C}^k = \int_{L^k}(\nabla_{pq}V,\mathbf{s})\,\mathrm{d}L; \tag{9}$$

where the side L^k has the nodes $n_{k\pm1/2}$, in the closed node sequence $k = 1,2,\ldots,M$ on the j-panel. For the computation of the contribution of $\tilde{C}^k$, we now impose a finite rotation of the planar dihedral p,q, in such way that the p-axis is parallel to the L^k side, so the ordinate $q = \text{cnst}$ during the side integration (see Fig. 2). The derivative of V along the direction of the planar unit vector $\mathbf{s}$ is computed as

$$(\nabla_{pq}V,\mathbf{s}) = \frac{\partial V}{\partial R}\frac{(\hat{\mathbf{R}},\mathbf{s})}{R}. \tag{10}$$

where $\nabla_{pq}R = \hat{\mathbf{R}}/R$ and $\hat{\mathbf{R}}$ is the unit vector in the radial direction R. Given the particular position of the local dihedral p,q in the L^k-side evaluation, we have $(\hat{\mathbf{R}},\mathbf{s}) = -q =$ cnst, and then

$$(\nabla_{pq}V,\mathbf{s}) = -\frac{q}{(R^2+\eta^2)^{1/2}} - \frac{q|\eta|}{[(R^2+\eta^2)^{1/2}-|\eta|](R^2+\eta^2)^{1/2}} + \frac{q|\eta|}{R^2}. \tag{11}$$

The monopolar integral along the L^k side is written as:

$$\tilde{C}^k = F(p_{k+1/2},q,\eta) - F(p_{k-1/2},q,\eta); \tag{12}$$

where $p_{k+1/2}, p_{k-1/2}$ are the extreme abscissas of the L^k side and q is the common ordinate, which are obtained as $p_{k\pm1/2} = (\mathbf{x}_{k\pm1/2}-\mathbf{x}_i)\cdot\mathbf{t}_k$ and $q = (\mathbf{x}_{k-1/2}-\mathbf{x}_i)\cdot\mathbf{s}_k$, where $\mathbf{t}_k, \mathbf{s}_k$ are the tangential and normal planar unit vectors of the L^k side on the panel surface. The sequence sense is such that $\mathbf{s}_k \times \mathbf{t}_k = \mathbf{n}_j$, where $\mathbf{n}_j$ is normal unit vector to the panel. The auxiliary function $F = F(p,q,\eta)$ is the sum:

$$F = -qF_1 - |\eta|qF_2 + |\eta|qF_3; \tag{13}$$

where the first integral is

$$F_1 = \int \frac{\mathrm{d}p}{\sqrt{p^2+(q^2+\eta^2)}} = \ln[p + \sqrt{p^2+(q^2+\eta^2)}]; \tag{14}$$

and the second one is

$$F_2 = \int \frac{\mathrm{d}p}{p^2+q^2} = \frac{1}{q}\tan^{-1}\left[\frac{p}{q}\right]. \tag{15}$$

For the third integral

$$F_3 = \int \frac{\mathrm{d}p}{[\sqrt{p^2+(q^2+\eta^2)}-|\eta|]\sqrt{p^2+(q^2+\eta^2)}}; \tag{16}$$

we introduce the variable change $p = \sqrt{q^2+\eta^2}\sinh\xi$, then:

$$F_3 = \int \frac{\mathrm{d}\xi}{\sqrt{q^2+\eta^2}\cosh\xi - |\eta|}; \tag{17}$$

with the solution [29]

$$F_3 = \frac{2}{q}\tan^{-1}\left[\frac{\sqrt{q^2+\eta^2}e^{\xi}-|\eta|}{q}\right]. \tag{18}$$

Now, we express $\xi(p)$ with

$$\sinh(\xi) = \frac{p}{\sqrt{q^2+\eta^2}} \equiv z; \tag{19}$$

then $y^2 - 2zy - 1 = 0$, where $y = e^{\xi}$, and its solution is $y = z \pm \sqrt{z^2+1}$. From this we obtain

$$e^{\xi}\sqrt{q^2+\eta^2} = p \pm \sqrt{p^2+q^2+\eta^2}. \tag{20}$$

It can be shown that the negative sign is the correct choice; then F_3 is written as

$$F_3 = \frac{2}{q}\tan^{-1}\left[\frac{p-|\eta|-\sqrt{p^2+q^2+\eta^2}}{q}\right]; \tag{21}$$

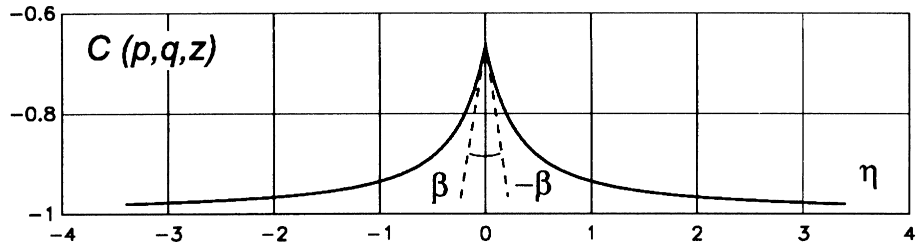

Fig. 3. Symmetry of the monopolar coefficient $\tilde{C}(p, q, \eta)$ with respect to the panel.

and the function F is

$$F = 2|\eta| \tan^{-1}\left[\frac{p - |\eta| - r}{q}\right] - q \ln[p + r]$$
$$- |\eta| \tan^{-1}\left[\frac{p}{q}\right]. \tag{22}$$

But, the sum by differences between the vertices of the L^k side of the function $\tan^{-1}(p/q)$ can be written as $\beta_k = \beta_{k+1/2} - \beta_{k-1/2}$, where

$$\beta_{k\pm1/2} = \tan^{-1}\left[\frac{p_{k\pm1/2}}{q_{k\pm1/2}}\right]; \tag{23}$$

where β^k is the view angle for the L^k side from the O local origin. Its sum over the closed perimeter is null and then this term will be omitted in F. We also note that the local origin O is the projection of the observation point $\mathbf{x}_i$ on the panel plane and is fixed during the integration. Then, the monopolar influence coefficient $\tilde{C}_{ij}$ between the j-source panel and the collocation point $\mathbf{x}_i$, is the sum of the M contributions

$$\tilde{C}_{ij} = \sum_{k=1}^{M} \tilde{C}^k \qquad \text{where}$$

$$\tilde{C}^k = F(p_{k+1/2}, q, \eta) - F(p_{k-1/2}, q, \eta); \tag{24}$$

where $p_{k\pm1/2}$ are its extreme abscissas and q the common ordinate, in the side dihedral p, q with p parallel to the L^k side. The (reduced) auxiliary function $F = F(p, q, n)$ is

$$F = 2|\eta|\tan^{-1}\left[\frac{p - |\eta| - \sqrt{p^2 + q^2 + \eta^2}}{q}\right]$$
$$- q \ln[p + \sqrt{p^2 + (q^2 + \eta^2)}]. \tag{25}$$

By direct computation we can verify the classical properties of the monopolar potential [1,2], for instance, let us consider the monopolar coefficient $\tilde{C}_{ij}$ as a function of the observation point p, q, η over a normal line passing through the panel centroid: (i) is a symmetrical function of the distance η between the observation point and the panel surface $\tilde{C}(p, q, \eta) = \tilde{C}(p, q, -\eta)$, and (ii) the tangents to the curve $\tilde{C}(p, q, \eta) = f(\eta)$ at the origin $\eta = 0$ are finites and the opposite sign, so the normal derivative $\partial\tilde{C}/\partial\eta$ has a finite jump to crossing the panel (Fig. 3). In Fig. 4 we show the monopolar intensity $\tilde{C}(p, q, \eta)$ for points (p, q, η) over the planes α parallel to the panel for two values of η.

5. Logarithmic singularity in the monopolar matrix

In the monopolar matrix **C** a singularity appears when both q and η vanish simultaneously, which is common, for instance, in flat-structured surfaces meshes as in ship-wave calculations, since all these panels are coplanar, so $\eta = 0$, and many of them will have side terms with $q = 0$, which can be arrived at by direct computation on a sample mesh, whereas the node coordinates from the projection point O are $p_1, p_2 > 0$ or $p_1, p_2 < 0$ for such flat-structured meshes (Fig. 5). The singularity is due to the logarithm term

$$\Delta b = \ln\frac{b_2}{b_1} = \ln\frac{p_2 + \sqrt{p_2^2 + q^2 + \eta^2}}{p_1 + \sqrt{p_1^2 + q^2 + \eta^2}}. \tag{26}$$

When $q = \eta = 0$, simultaneously, we have

$$\Delta b = +\ln\frac{p_2 + |p_2|}{p_1 + |p_1|} \qquad \text{for } p_1, p_2 > 0; \tag{27}$$

which is a regular term. But, when $p_1, p_2 < 0$ we have $\Delta b = NaN$ (undefined). In order to overcome this shortcoming, we employ the classical technique of subtracting the

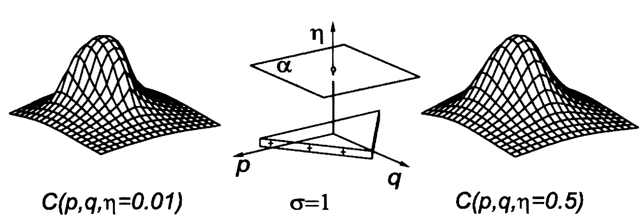

Fig. 4. Intensity of the monopolar coefficient $\tilde{C}(p, q, \eta)$ over the planes α, for: $\eta = 0.01$ (left) and $\eta = 0.50$ (right).

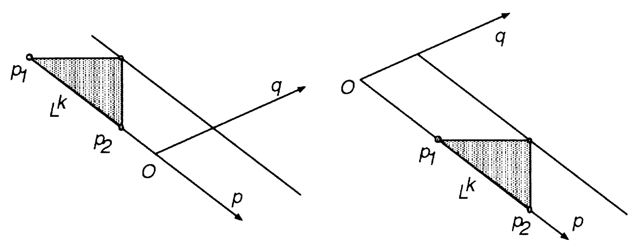

Fig. 5. The cases $p_1, p_2 < 0$ (left) and $p_1, p_2 > 0$ (right), both with $q = \eta = 0$.

singularity, i.e.

$$\Delta b \equiv \ln \left\{ \frac{p_2 + r_2}{p_1 + r_1} \frac{r_2 - p_2}{r_1 - p_1} \frac{r_1 - p_1}{r_2 - p_2} \right\}; \tag{28}$$

where $r_{1,2}^2 = p_{1,2}^2 + q^2 + \eta^2$ so that

$$\Delta b = \ln \left\{ \frac{r_2^2 - p_2^2}{r_1^2 - p_1^2} \frac{r_1 - p_1}{r_2 - p_2} \right\}; \tag{29}$$

but $r_2^2 - p_2^2 = r_1^2 - p_1^2 = q^2 + \eta^2$; then

$$\Delta b = -\ln \frac{\sqrt{p_2^2 + q^2 + \eta^2} - p_2}{\sqrt{p_1^2 + q^2 + \eta^2} - p_1}. \tag{30}$$

When $q = \eta = 0$, simultaneously we have

$$\Delta b = -\ln \frac{|p_2| - p_2}{|p_1| - p_1} \qquad \text{for } p_1, p_2 < 0. \tag{31}$$

Both Eqs. (27) and (31) can be reduced to

$$\Delta b = \ln \frac{b_2}{b_1} = \operatorname{sgn}(p_1) \ln \frac{|p_2|}{|p_1|} \qquad \text{for } q = \eta = 0. \tag{32}$$

From a computational viewpoint, we suppose that $q = \eta = 0$ is present when the condition $\sqrt{q^2 + \eta^2} < \varepsilon \max\{|p_1|, |p_2|\}$ is verified, where ε is a fixed tolerance.

6. Dipolar matrix

The dipolar matrix $\tilde{A}_{ij}$ is found from

$$\tilde{A}_{ij} = \int_{S_j} \mathrm{d}\Gamma_y \frac{\partial}{\partial_{n_y}} \frac{1}{r}; \tag{33}$$

where ∂_n is the normal derivative to the surface panel. The dipolar kernel $\partial_{n_y} r^{-1}$ can be expressed as

$$\frac{\partial}{\partial n} \frac{1}{r} = \frac{\partial}{\partial r} \frac{1}{r} \frac{\partial r}{\partial n} = \frac{-1}{r^2} \frac{\eta}{r} = -\frac{\eta}{r^3} \tag{34}$$

Again we employ the previous strategy: we find an auxiliary function $W(R, \eta)$ such that its bidimensional Laplacian $\Delta_{pq} W$ over the panel surface is equal to the dipolar kernel $-\eta/r^3$, i.e.

$$\Delta_{pq} W = -\frac{\eta}{r^3}; \tag{35}$$

Then, the surface integral is replaced by the line integral by means of the 2D-divergence theorem

$$\tilde{A}_{ij} = \int_{S_j} \Delta_{pq} W \, \mathrm{d}S_{pq} = \int_{L_j} (\nabla_{pq} W, \mathbf{s}) \, \mathrm{d}L; \tag{36}$$

where $W(R, \eta)$ is a regular enough function which is found from the solution of the differential equation

$$\frac{1}{R} \frac{\partial}{\partial R} \left(R \frac{\partial W}{\partial R} \right) = -\frac{\eta}{\{R^2 + \eta^2\}^{3/2}}; \tag{37}$$

where $\Delta_{pq} W$ is the bidimensional Laplacian in the R, θ polar coordinates, with $\partial_\theta W = 0$. The integration gives:

$$W = \int \frac{\eta}{R\sqrt{R^2 + \eta^2}} \mathrm{d}R; \tag{38}$$

which admits the solution [32]

$$W = \frac{\eta}{|\eta|} \ln \left[\frac{\sqrt{R^2 + \eta^2} - |\eta|}{R} \right] \qquad \text{for } R > 0; \tag{39}$$

where the logarithm argument is positive for R, η positives. Then, the line integral for the monopolar coefficient $\tilde{A}_{ij}$ can be written as the sum of the $\tilde{A}^k$ contributions of the surface gradient of the auxiliary dipolar function W

$$\tilde{A}_{ij} = \sum_{k=1}^{M} \tilde{A}^k \qquad \text{where} \qquad \tilde{A}^k = \int_{S^k} (\nabla_{pq} W, \mathbf{s}) \, \mathrm{d}L; \tag{40}$$

The s component of the gradient ∇W is

$$(\nabla_{pq} W, \mathbf{s}) = \frac{\partial W}{\partial R} \frac{(\hat{\mathbf{R}}, \mathbf{s})}{R}; \tag{41}$$

due the position of the local dihedral p, q for the L^k side we

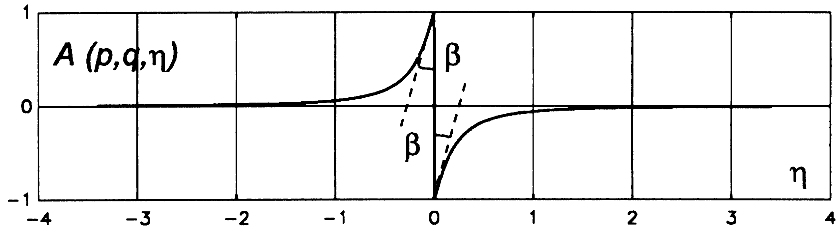

Fig. 6. Skew-symmetry of the dipolar coefficient $\tilde{A}(p, q, n)$ with respect to the panel.

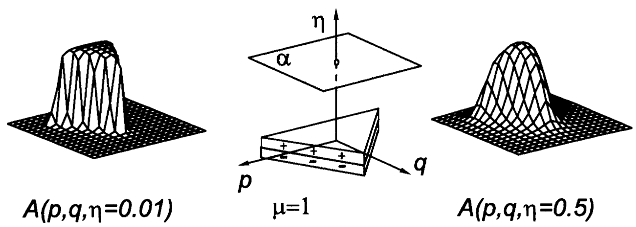

Fig. 7. Intensity of the dipolar coefficient $\tilde{A}(p,q,\eta)$ over the planes α, for: $\eta = 0.01$ (left) and $\eta = 0.5$ (right).

have $(\hat{\mathbf{R}}, \mathbf{s}) = -q = \text{cnst}$. Then

$$(\nabla_{pq} W, \mathbf{s}) = q\,\mathrm{sgn}(\eta)\frac{1}{[\sqrt{R^2+\eta^2} - |\eta|]\sqrt{R^2+\eta^2}} - q\,\mathrm{sgn}(\eta)\frac{1}{R^2}. \quad (42)$$

The dipolar lineal integral on the L^k side, is written as

$$A^k = D(p_{k+1/2}, q, \eta) - D(p_{k-1/2}, q, \eta); \quad (43)$$

where the auxiliary dipolar function $D(p,q,\eta)$ is the sum

$$D = q\,\mathrm{sgn}(\eta) D_1 - q\,\mathrm{sgn}(\eta) D_2. \quad (44)$$

The integral D_1 is the same as the monopolar F_3. The integral D_2 is equal to the monopolar term F_2, so its closed sum around the panel perimeter is null. Then, the dipolar influence coefficient $\tilde{A}_{ij}$ between the j-source panel and the collocation point $\mathbf{x}_i$, is the sum of the M contributions

$$\tilde{A}_{ij} = \sum_{k=1}^{M} \tilde{A}^k \qquad \text{where}$$

$$\tilde{A}^k = D(p_{k+1/2}, q, \eta) - D(p_{k-1/2,} q, \eta); \quad (45)$$

where

$$D = 2\,\mathrm{sgn}(\eta)\tan^{-1}\left[\frac{p - |\eta| - \sqrt{p^2+q^2+\eta^2}}{q}\right]. \quad (46)$$

Again, by direct computation we can verify the classical properties of the dipolar coefficient [1,2]. For instance, let us consider the monopolar coefficient $\tilde{A}_{ij}$ as a function of the observation point p, q, η over a normal line passing trough the panel centroid: (i) is a skew-symmetric function of the distance η between the observation point and the panel surface $\tilde{A}(p,q,\eta) = -\tilde{A}(p,q,-\eta)$, and (ii) the tangents to the curve $\tilde{A}(p,q,\eta) = f(\eta)$ at the origin $\eta = 0$ are finites and with the same sign, so the normal derivative $\partial_n \tilde{A}$ remains continuous when crossing the panel (Fig. 6). In Fig. 7 we show the dipolar intensity $\tilde{A}$ for points over the planes α parallel to the panel for two values of η.

Acknowledgements

This work has received financial support from CONICET (Argentina) through grant BID 802/OC-AR PID Nr. 26, and from UNL (Argentina).

References

[1] Katz J, Plotkin A. Low-speed aerodynamics, from wing theory to panel methods. New York: McGraw-Hill, 1991.
[2] Hunt B, editor. Numerical methods in applied fluid dynamics New York: Academic Press, 1980.
[3] Sclavounos PD. Computation of wave ship interactions. Advances in marine hydrodynamics. Boston, MA: Computational Mechanics Publications, 1996.
[4] Larson L, Baba E. Ship resistance and flow computation. Advances in marine hydrodynamics. Boston, MA: Computational Mechanics Publications, 1996.
[5] Mokry M. Complex variable boundary element method for external potential flows. 28th Aerospace Sciences Meeting, 8–11 January, Reno, NV 1990.
[6] Storti M, D'Elía J, Idelsohn S. CVBEM formulation for multiple profiles and cascades. Appl Mech Rev 1995;48(11):203–10.
[7] Hess JL. Review of integral-equation techniques for solving potential-flow problems with emphasis on the surface-source method. Comput Meth Appl Mech Engng 1975;5:145–96.
[8] Richarson T, Katz JC, Ashby DL. Unsteady panel method for flows with multiple bodies moving along various paths. AIAA J 1994;32:62–8.
[9] Larson L, Broberg L, Kim KJ, Zhang DH. New viscous and inviscid CFD techniques for ship flow. Fifth International Conference on Numerical Ship Hydrodynamics, Hiroshima, Japan, September, 1989. p. 1–25.
[10] Ohkusu M. Hydrodynamics of ships in waves. Advances in marine hydrodynamics. Boston, MA: Computational Mechanics Publications, 1996.
[11] Nakos D.E. Sclavounos, P.D. Ship motions by a three dimensional Rankine panel method. Proceedings of the 18th Symposium on Numerical Ship Hydrodynamics, Iowa 1990.
[12] Dawson CW. A practical computer method for solving ship-wave problems. Second International Conference on Numerical Ships Hydrodynamics, Berkeley, CA, 1977. p. 30–8.
[13] Korsmeyer FT, Bingham H. The forward speed diffraction problem. J Ship Res 1998;42(2):99–112.
[14] Huang Y, Sclavounos PD. Nonlinear ship motions. J Ship Res 1998;42(2):120–30.
[15] Kring DC. Ship seakeeping through the $\tau = 1/4$ critical frequency. J Ship Res 1998;42(2):113–998.
[16] Korsemeyer FT, Sclavounos PD. The large-time asymptotic expansion of the impulse response function for a floating body. Appl Ocean Res 1989;11(2):75–88.
[17] Broeze J, Van Daalen EFG, Zandbergen PJ. A three-dimensional panel method for nonlinear free surface waves on vectors computers. Comput Mech 1993;13:12–28.
[18] Sierevogel L. Time-domain calculations of ship motions. PhD thesis, Technische Universiteit Delft, 1998.
[19] Prins HJ. Time-domain calculations of drift forces and moments. PhD thesis, Technische Universiteit Delft, 1995.
[20] Liapis SJ. Time-domain analysis of ship motions. PhD thesis, University of Michigan, 1986.
[21] Nakos D.E, Kring D.C. Sclavounos P.D. Rankine panel methods for transient free surface flows. Proceedings of the Sixth International Conference on Numerical Ship Hydrodynamics, Iowa 1993.
[22] Beck R.F, Cao Y, Lee T.H, Fully nonlinear time-domain computation of waterwave problems using the desingularized method. Proceedings of the Sixth International Conference on Numerical Ship Hydrodynamics, Iowa 1993.
[23] Hsin CY. Development and Analysis of Panel Methods for Propellers

in Unsteady Flow, Report 91-1. Boston, MA: Departament of Ocean Engineering, Massachusetts Institute of Technology, 1991.

[24] Morino L, editor. Computational methods in potential aerodynamics Berlin: Springer, 1985.

[25] Morino L, Kuo CC. Subsonic potential aerodynamics for complex configurations: a general theory. AIAA J 1974;12:191–7.

[26] Newman JN. Distributions of sources and normal dipoles over a quadrilateral panel. J Engng Math 1986;20:113–26.

[27] Medina DE, Liggett JA. Three-dimensional boundary element computation of potential flow in fractured rock. Int J Numer Meth Engng 1988;26:2319–30.

[28] D’Elía J. Numerical methods for the ship wave-resistance problem. PhD thesis, Universitie Nacional del Litoral, Santa Fe, Argentina, 1997.

[29] Storti M, D’Elía J, Idelsohn S. Algebraic discrete non-local (DNL) absorbing boundary condition for the ship wave resistance problem. J Comput Phys 1998;146(2):570–602.

[30] Storti M, D’Elía J, Idelsohn S. Computing ship wave resistance from wave amplitude with the DNL absorbing boundary condition. Common Numer Meth Engng 1998;14:997–1012.

[31] D’Elía J, Storti M, Idelsohn S. A panel-Fourier method for free surface methods. ASME J Fluids Engng in press.

[32] Spiegel MR. Mathematical Handbook. New York: McGraw-Hill, 1968.